

# Landslides triggered by the Ms 7.0 Lushan earthquake, China

X. L. CHEN<sup>1</sup>, L. YU<sup>1</sup>, M. M. WANG<sup>2</sup>, C. X. LIN<sup>3</sup>, C. G. LIU<sup>4</sup> and J. Y. LI<sup>1</sup>

1 Key lab of active tectonics and volcano, Institute of Geology, China Earthquake Administration, Beijing, 100029, China

2 Earthquake Administration of Sichuan Province, Chengdu, 610041, China

3 Beijing Institute of Geology, Beijing, 100120, China

4 China Earthquake Networks Center, Beijing, 100045, China

## Abstract

Earthquake-triggered landslide has drawn much attention in the world because of severe hazards it causes. The Ms 7.0 Lushan earthquake, occurred in the Longmen Shan mountain region in Sichuan Province of China on April 20, 2013, triggered more than 1,000 landslides and really blocked many roads and exacerbated the overall transportation problems in the mountainous region. Preliminary landslides inventory is compiled based on the high-resolution remote sensing images. Based on it, landslides spatial distribution characteristics and correlations between the occurrence of landslides and geologic and geomorphologic conditions are analyzed. Meanwhile, statistic analysis is conducted using landslide point density (LPD), which is defined as the number of landslides per square kilometer. It is found that LPD has strong positive correlation with slope gradients, and the higher LPD occur in younger strata systems like Quaternary and Tertiary sediments in this study area. Spatially, the triggered landslides are controlled by the causative faults and mainly concentrate around the epicenter. All the landslides are located within the area with seismic intensity  $\geq$  VII and in scale with the seismic intensity. Generally, LPD decreases with increasing distance from the epicenter, and sometimes landslides are densely distributed along the roads in the mountainous region. It is found that the empirical distance-magnitude relation is more suitable for estimating the landslides concentrated area during the Lushan earthquake.

Key words: the Lushan earthquake, spatial distribution, landslides, landslide point density (LPD), landslides affected area

## 1 Introduction

At 08:02 (Beijing Time) on 20 April 2013, a strong earthquake with Ms 7.0 in surface wave magnitude occurred at the eastern margin of the Tibetan Plateau in Sichuan province, China. Its focal depth is of 13 km (<http://www.cea.gov.cn/publish/dizhenj>). The event is named the Lushan earthquake as its epicenter (30.3°N and 103.0°E) is located in the administrative region of Lushan County (Fig. 1). According to the government report, there are 196 people killed in this event.

The Ms 7.0 Lushan earthquake occurred in the Longmen Shan mountain range, where did a

catastrophic earthquake named the Wenchuan earthquake occur 5 years ago. This recent earthquake occurred at the south side of the Wehchuan earthquake, the distance between these two earthquakes is around 90 km.

As it is known that strong earthquakes can trigger lots of landslides in the mountainous area, the Lushan earthquake is no exception. Preliminary remote sensing images interpretation and field investigation show that there are more than 1,000 landslides triggered during this earthquake, ranging in the size from rock falls to rock avalanches with several ten thousands of cubic meters. Compared with the Wenchuan earthquake, the landslides triggered by the Lushan earthquake are smaller both in the amount and the affected area.

The phenomenon that such two strong earthquakes occurred in the Longmen Shan fault zone (LSFZ) in 5 years, attracts the scientists not only to explore the relation between them, but also to study the geohazards caused by the Lushan earthquake.

In this study, we analyze the spatial distribution characteristics of landslides triggered by the Lushan earthquake and investigate correlations between the occurrence of landslides and geologic and geomorphologic conditions by correlating landslide-point density (LPD) with the factors influencing stability of slopes during a seismic event. LPD is defined as the number of landslides per square kilometer and it is widely used in landslides statistic analysis (Wang et al., 2007; Dai et al., 2011). Meantime, we conclude in a discussion that distance-magnitude relation can be more suitable for estimating the landslides concentrated area by the Lushan earthquake. Also, in order to effectively evaluate the landslide hazard severity, interpretation standards for delimitating landslides are expected.

## 2 Tectonic setting

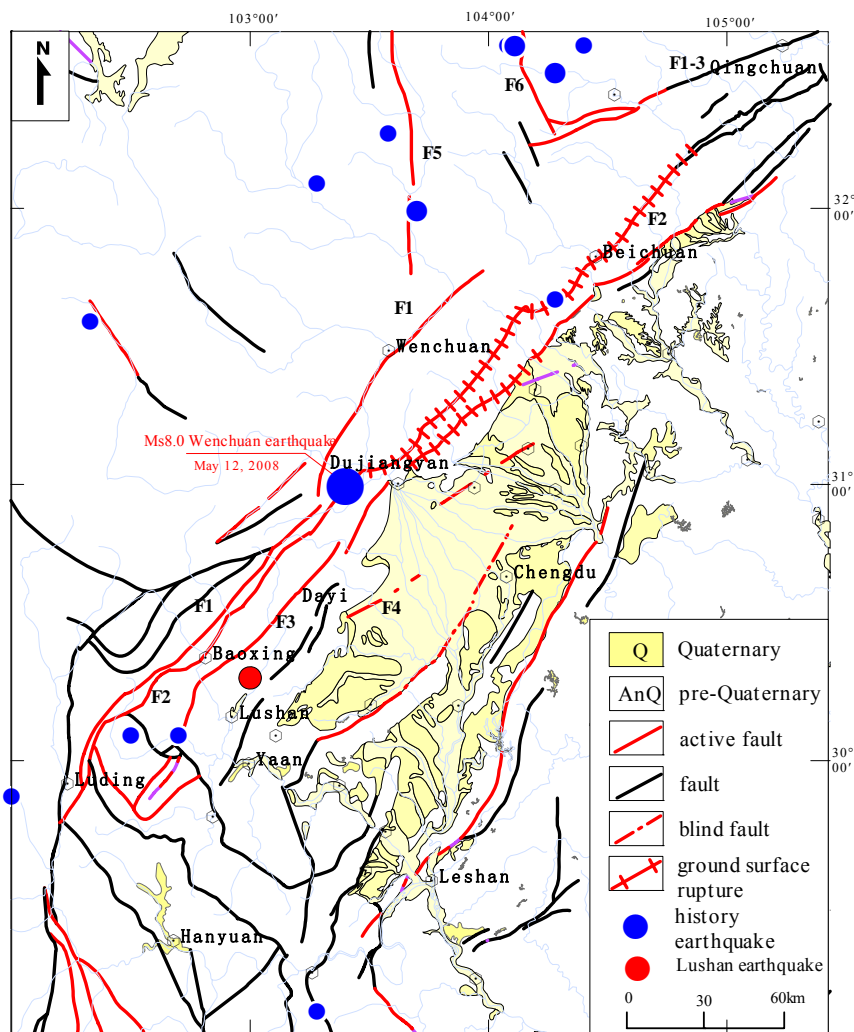
The Ms7.0 Lushan earthquake occurred at the southern segment of the Longmen Shan fault zone (LSFZ) in the eastern margin of the Tibetan Plateau. The LSFZ, which strikes approximately N45°E and dips at 50°–75° toward the northwest (Xu et al., 2008), lies along the middle segment of the Central Longitudinal Seismic Belt (CLSB) of China, and separates the seismically active Tibetan Plateau from the tectonically stable Ordos block, Sichuan basin, and South China block (Zhang et al. 2010). It consists of three sub-parallel thrust faults, namely the Wenchuan-Maowen (F1), Yingxiu-Beichuan (F2), and Guanxian-Anxian (F3) faults, and a frontal blind thrust fault (F4). During the 2008 Wenchuan earthquake, the event ruptured several strands of this fault zone, and the primary rupture is on the Yingxiu-Beichuan strand (Xu et al., 2008). Except for these 3 main faults in the LSFZ, there are others faults and folds developed in this region during the geological evolution (Fig. 1).

The Longmen Shan mountain range is deforming as a result of the collision between the Indian plate and the Eurasian plate. It resulted in structural stress accumulation on the collision edges and later, release of stress in the fault zone brought on a catastrophic earthquake named the Wenchuan earthquake in 2008. As the Wenchuan earthquake, the Lushan earthquake is also a strong earthquake caused by the slipping of slightly dipping abnormal faults in the deep of the southern part of Longmenshan nappe structure zone. The epicenter of the Lushan earthquake is located in the area with increasing Coulomb stress, so that the occurrence of the Wenchuan earthquake may trigger or accelerate the Lushan earthquake ( Xu et al., 2013).

Unlike the Wenchuan earthquake, which generated long ground surface ruptures, the field investigation after the Lushan earthquake indicated that although there are some fracture evidences at the surface, no obvious surface fracture zones are formed (Han et al., 2013). Combining spatial distribution of the relocated aftershocks and focal mechanism solutions, it is inferred that the Lushan earthquake is classified as a typical blind reverse-fault earthquake (Xu et al. 2013).

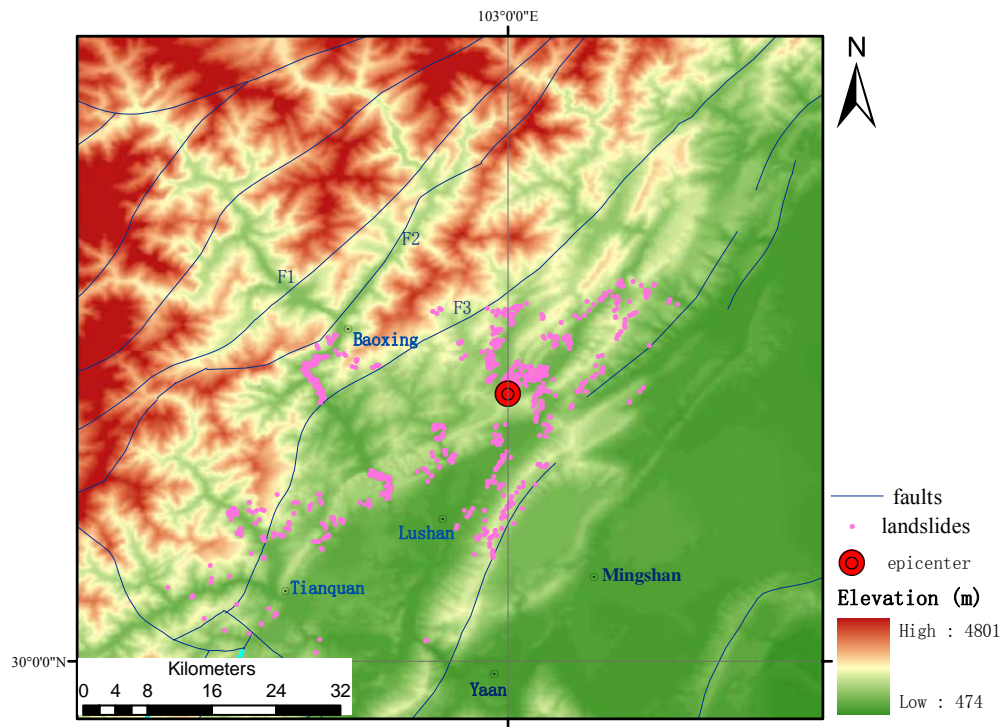
Topographically, as the transitional zone from the Tibetan Plateau to the Sichuan Basin plain, the relief in the Longmen Shan mountain range gradually decreases eastward. To its west, elevations reach more than 4000 m above sea level, while at east of this belt, the elevation of the Sichuan basin lies only 600 m above sea level. On the whole, elevation at the northwestern region is higher than at the southeastern as well as the relief in northwestern side is steeper than in southeastern side. In the study region, the elevation is mainly lower than 3000 m (Fig. 2).

The steep western margin of the Sichuan basin is known to be seismically active. Frequent regional tectonic activities have created a topography presenting high mountains intersected by deep incised valleys and developed a geologically weak region with fragile strata. Therefore, this region is notoriously prone to landslide. Pre-paleozoic to Cenozoic rocks and Quaternary sediments crop out in the region (Fig. 1, Fig. 6).



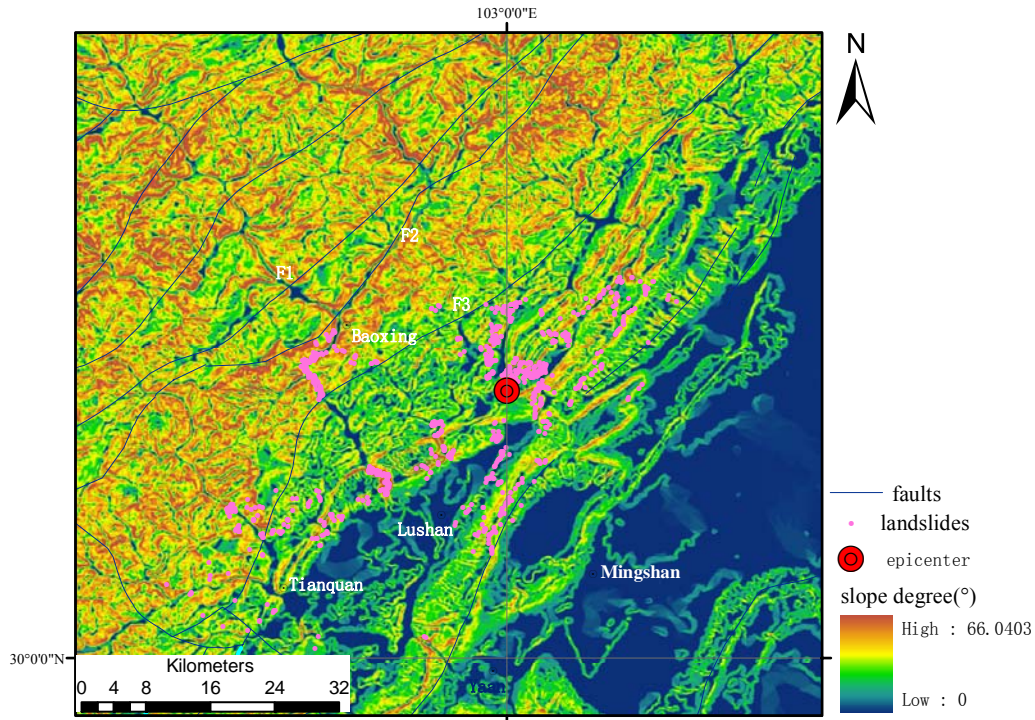
F1: Wenchuan-Maowen fault, F2: Yingxiu-Beichuan fault, F3: Guanxian-Anxian fault, F4: frontal blind fault,  
F5: Minjiang fault, F6: Huya fault

**Fig. 1.** Geological map for the Lushan earthquake and adjacent region



**F1: Wenchuan-Maowen fault, F2: Yingxiu-Beichuan fault, F3: Guanxian-Anxian fault**

**Fig. 2.** Elevation map for the study region and the landslides triggered by the Lushan earthquake



**F1: Wenchuan-Maowen fault, F2: Yingxiu-Beichuan fault, F3: Guanxian-Anxian fault**

Fig. 3. Slope map for the study region and the landslides triggered by the Lushan earthquake

### 3 Lushan earthquake-Triggered Landslides

The occurrence of earthquake-triggered landslides is generally related to the magnitude of ground motion, the distance from an earthquake fault, rock characteristics, slope gradient and so on (Harp et al., 1981; Keefer, 1984; Wang et al., 2003; Jibson et al., 2004; Meunier et al., 2007; Wang et al., 2007; Qi et al., 2010; Dai et al., 2011; Catani et al., 2013). The Lushan earthquake-triggered landslides provide a good opportunity to discuss some factors that influence effectively on landslides occurrence.

As a whole, the landslides spread in the NE-SW extending direction the same as the LSFZ, showing the influence from the tectonics. Because the southwestern region of the epicenter is occupied by an intermountain basin, landslides distribution is absent in the inner basin while continue distributing along the basin sides (Fig. 3). Landslides inventory map as well as field investigation shows that the area seriously affected by the landslides is limited to the epicentral region (Fig. 2, Fig. 3). Away from the epicenter, the landslides scatter and present mainly in the form of rock falls.

#### 3.1 Types of landslides

Base on the field investigation, it is found that the landslides triggered by the Lushan earthquake appear mainly in the forms of rock falls (Fig. 3a), shallow slope failures (Fig. 3b) and rock or soil slides (Fig. 3c). This definition is in accordance with "The landslide handbook—A guide to understanding landslides" (Highland, L.M., and Bobrowsky, Peter, 2008). Rock falls commonly



occur on steep slopes or along rocky banks of rivers and roads, with small volume of several to tens thousands cubic meters. Shallow slopes failures are composed of weathered and fractured materials, appearing on gentle to moderate slopes. Rock or soil slides generally have a slide plane which is on surfaces of rupture or on relatively thin zones of intense shear strain. This kind of landslide always can make severe damage because of their big volumes.



(a) Rock falls (photo taken by Dr. M.M. Wang)



(b) Shallow slope failures (photo taken by Dr. M.M. Wang)



(c) Rock slides (photo taken by Dr. M.M. Wang)

Fig. 4. Landslides during the Lushan earthquake

### 3.2 Landslides inventory

Landslide inventory is an essential part of seismic landslides hazard analysis (Harp et al., 2011; Guzzetti et al., 2012). Compared with traditional landslide inventory compilation, landslide detection and mapping now benefit from both optical and radar imagery. Many studies and researches on landslides have proved that remote sensing can be considered as a powerful instrument for landslides mapping, monitoring and hazard analysis (Qi et al., 2010; Dai et al., 2011; Tofani et al., 2013; Xu et al., 2013). For the Lushan earthquake, remote sensing (RS) technology is playing a vital role in accessing the information in quake disaster areas.

In our study, compilation of landslide inventories is mainly performed by means of interpretation of aerial photography. Because most landslides triggered by the Lushan earthquake have small size both in plane area and volume, it is a better way to map landslides as points which represent the failure sources near the top scarps. Similar to Dr. Dai (Dai et al., 2011), landslides were identified in the remote sensing images by the following characteristics: (1) landslides scarps showed newly denuded vegetation on the slopes; (2) landslides scarps showed distinct white or brown contrast as compared to the surrounding; (3) landslide debris movement paths could be clearly observed; (4) Individual boulders rock falls are not accounted in this study.

The remote sensing images used in this study are with resolution of 0.6 m. Except for the regions covered by the clouds and shadows, landslides can be detected easily from the images in the majority of the study region. Totally, there are 1129 landslides mapped and the affected area is around 2200 km<sup>2</sup> (Fig. 2, Fig. 3, Fig. 9). Following analysis of correlating LPD with the factors influencing stability of slopes is based on this affected area.

### 3.3 Variation of landslide distribution with slope gradient

Many researches show that topographic features can affect landslide distribution (Qi, 2006; Keefer, 1984, 2006; Dai et al, 2011; Catani et al., 2013). In general, steeper and higher slopes are more prone to landslide activity than gentle slopes. In this study, DEM (SRTM, 90m) was used to generate slope angles, and then slope angles were reclassified at intervals of 5°. Because the areas with slope gradient greater than 45° together cover less than 2% of the total surface area, they are classified as one category. The relationship between landslides and the corresponding slope gradient categories has been examined as shown in Fig. 5. It is shown that LPD values steadily increase with slope angles.

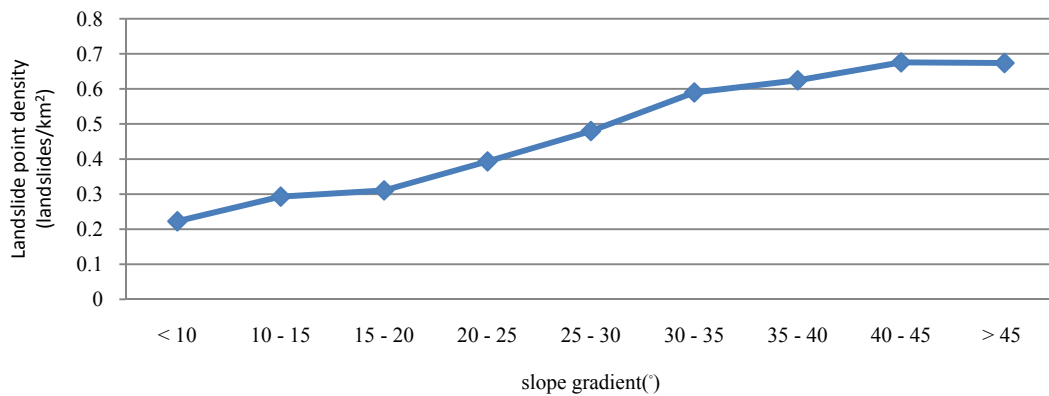


**Fig. 5.** Landslide point density vs. slope degree

### 3.4 Landslide concentration with geological formations

The damaged area is mainly composed of Mesozoic and Cenozoic strata, which crop out in the eastern side of the region (Fig. 6). Paleozoic and pre-Paleozoic sediments are limited to the northwestern side of the region with higher and steeper relief (Fig. 2, Fig. 3). Studies on the landslides distribution show that most of the landslides are presented in the Cretaceous strata, which consist of siltstone, mudstone, or mudstone intercalated with shale. These rocks are heavily fractured and always have weak shear strength. So it is found that most of landslides concentrated on the slopes consisting of such rocks. Tertiary and Quaternary sediments present near the epicenter in a comparatively flat plain, therefore, landslides frequently occurred here despite the relief is generally gentle without steep slopes. In order to understand the strata system of the area, a simplified strata system is shown in table 1.



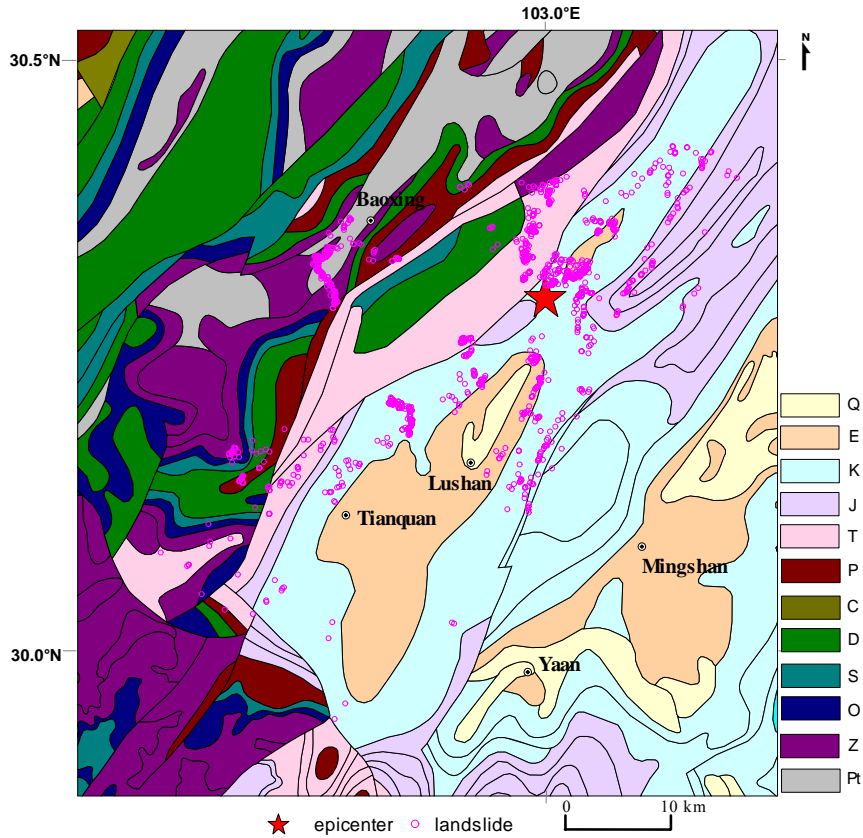


**Fig. 6** Geological map for the damaged region by the Lushan earthquake (revised after CGS, Regional geological map of Sichuan Province (1:200, 000), 2001)

**Table 1. Simplified geologic strata system of the area most severely damaged by the Ms 7.0 Lushan earthquake**

Sequence	Symbol	Lithology
Quaternary	Q	Alluvium, Loose deposit
Tertiary	E	Mudstone, sometimes intercalated with mudstone
Cretaceous	K	Conglomerate
Jurassic	J	Sandy slate, mudstone, sandy stone intercalated with mudstone
Triassic	T	Sandy stone, limestone, slate
Permian	P	Thick limestone intercalated slate
Carboniferous	C	Limestone, marble and sandy stone
Devonian	D	Quartzose sandstone
Silurian	S	Sandy stone, phyllite intercalated with limestone
Ordovician	O	Limestone, marble and phyllite of Baota formation
Sinian	Z	Metamorphic sandy stone, metamorphic limestone
Archean	Pt	Granite, diorite, gabbro

Except for Triassic sediments, LPD value decreases with the strata turning old (Fig. 7). The highest LPD is in the Quaternary system. Though there are not many landslides (< 30) occurred in the Quaternary system, the LPD is high because of this stratum's small area of 20 km<sup>2</sup>. Without

regarding to the area with slope degree lower than 10° in different strata systems, the bigger LPD value appears in the Quaternary and Tertiary sediments. Considering the epicenter location in the geological setting (Fig.3, Fig.6), it is reasonable that the landslides concentrated in the area around the epicenter with steeper relief and softer materials.

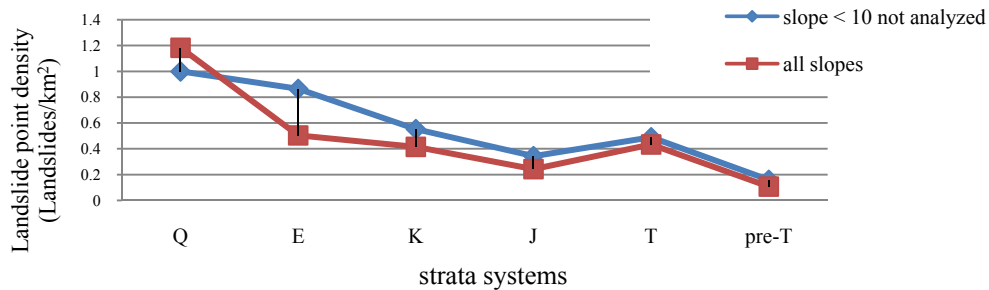


**Fig.7.** Landslide point density vs. strata systems

### 3.5 Distribution of landslides with the distance to epicenter and seismic intensity

Causative fault is an important factor that can influence the distribution of landslides during a strong shaking event (Khazai and Sitar, 2003; Wen et al., 2004; Wang et al., 2008; Catani et al., 2013). With the increasing of the distance from the causative fault or epicenter, the number of triggered landslides presents a negative-exponential decline (Simonett, 1967; Keefer, 2000; Wang et al., 2007).

The Ms7.0 Lushan earthquake is caused by a blind thrust fault, however, there is no obvious surface rupture found during the field investigation which was conducted by the Institute of Geology, China Earthquake Administration sooner after the earthquake ([http://www.eq-igl.ac.cn/wwwroot/c\\_000000090002/d\\_0976.html](http://www.eq-igl.ac.cn/wwwroot/c_000000090002/d_0976.html)). This leads to the seismic causative fault an unresolved matter at present.

In this study, the distance to the epicenter is used to analyze the landslides variation. LPD is calculated by 5 km intervals circle buffer centered at the epicenter. The analysis result shows that LPD value decreases with the increasing distance to the epicenter. More than 90% of the landslides are located within 30 km from the epicenter.

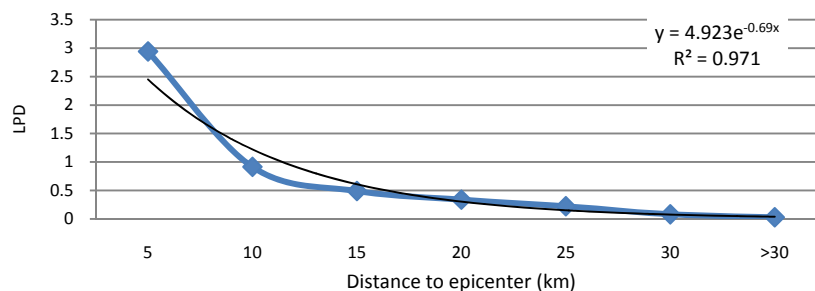
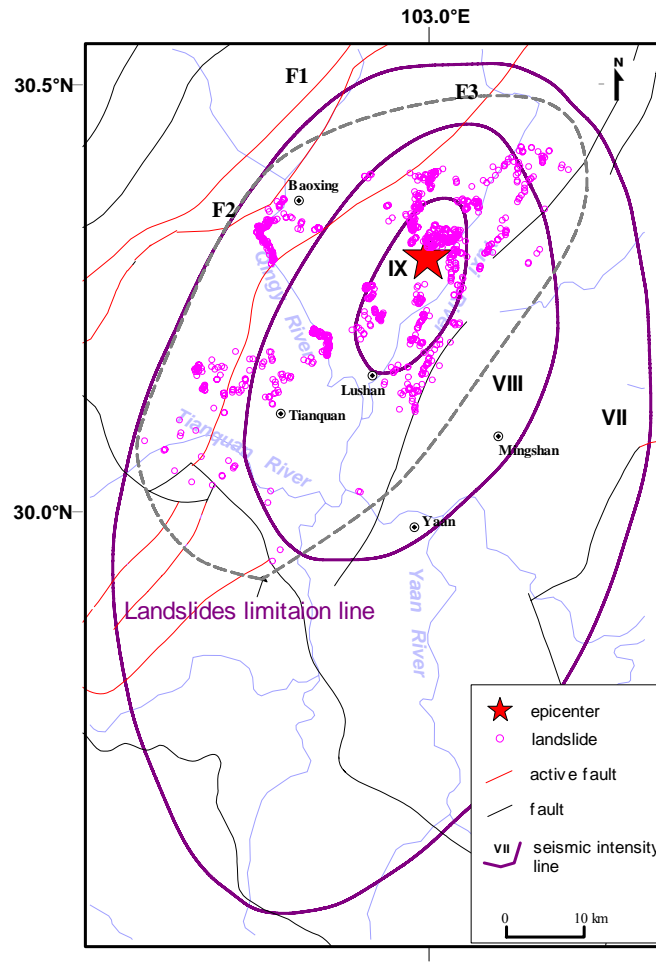


Fig. 8. Landslides distribution with the distance from the epicenter

Based on the 4.20 Lushan earthquake seismic intensity distribution map issued by China Earthquake Administration ( [http : //www.cea.gov.cn/publish/dizhenj/464](http://www.cea.gov.cn/publish/dizhenj/464)), it is found that all the landslides are located within the area with seismic intensity  $\geq$  VII. The analysis results indicate that the landslides number is in scale with seismic intensity (Fig. 9). In the epicentral region with seismic intensity of IX, the LPD value reaches  $1.72/\text{km}^2$ , which is many times greater than that in the region with seismic intensity of VII (Fig. 10).



F1: Wenchuan-Maowen fault, F2: Yingxiu-Beichuan fault, F3: Guanxian-Anxian fault

Fig. 9. Seismic intensity distribution and the landslides limitation line

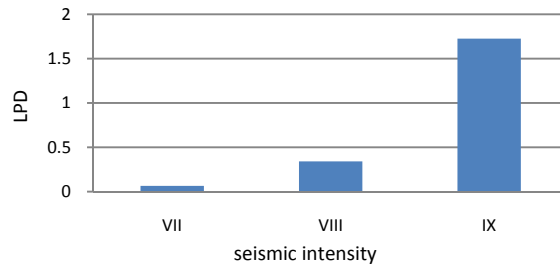
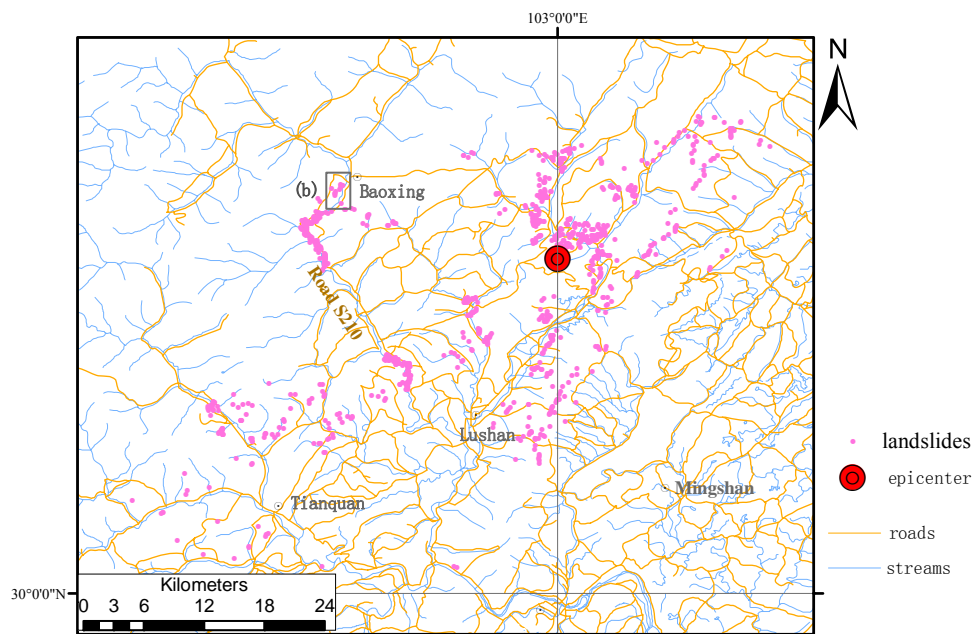


Fig. 10. LPD variation with seismic intensity

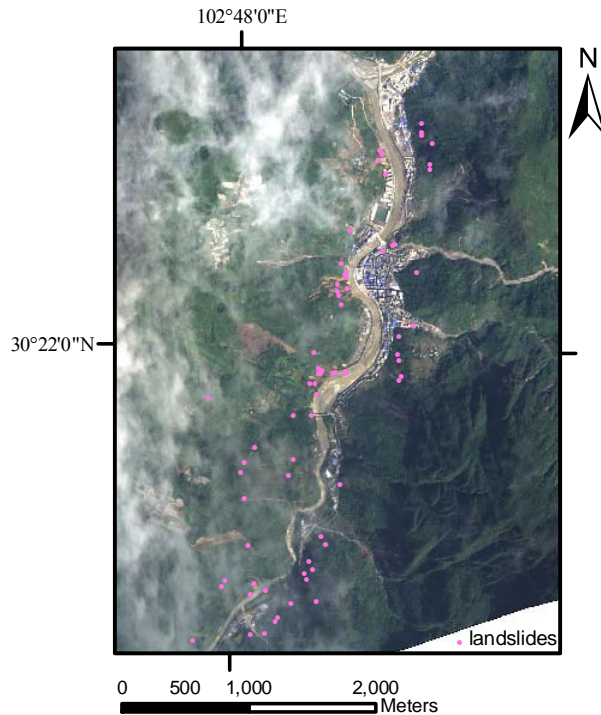
### 3.6 Distribution of landslides along the roads

As a landslide predisposing factor, road or distance to road has been successfully used in landslide susceptibility assessments (Devkota et al., 2013; Ramakrishnan et al., 2013; Catani et al., 2013).

Due to geographical conditions in the study region, many landslides develop densely along the roads in the mountainous area and river banks (Fig. 11). For example, there are 79 landslides occurred in a 5 km length of Road S210 near the Baoxing County (Fig. 11). In fact, it is a normal phenomenon that landslides are likely to occur along roads or rivers bank in the southwest China, and a strong seismic event will definitely aggravate this kind geohazards and usually generate landslides dams on the river systems. This phenomenon reveals that the man-made roads in the mountainous area had modified the hill slope profile, and became an important factor to influence the landslides occurrence.



(a) Landslides distribution with the roads and streams



(b) Remote image of the landslides along the road near Baoxing County (location is indicated in (a); Image provided by the Institute of Remote Sensing and Digital Earth, China Academic Science)

Fig. 11. Landslides distribution with the roads and streams

## 4. Discussions

### 4.1 Estimation of the area affected by landslides

The area affected by earthquake-triggered landslides shows strong correlation with earthquake magnitude, and earthquakes with bigger magnitude can cause wider influencing area (Keefer, 1984; Bommer et al, 2002; Rodríguez et al, 1999). Therefore, seismic magnitude and the distance from the epicenter or the causative seismic fault are usually used to judge the limitation boundary of the landslides affected area.

1. Kawabe et al. (2000) suggested that the maximum distance ( $D$ ) from epicenter to landslide can be calculated using following equation:

$$\log D = 0.5M - 2.0 \quad (1)$$

where  $M$  is the seismic magnitude,  $D$  is the distance in unit of km.

For the Lushan earthquake, after substituting 7.0 for  $M$  in the equation (1), we obtain  $D = 31.6$  km, which is very close to the distance calculated from the landslide inventory, and it is also within the semi-minor axis (33 km) of seismic intensity VII (Fig. 9). Although the maximum distance in the Lushan earthquake is around 45 km, our analysis results show that more than 90% of the landslides are located within 30 km from the epicenter.



2. In Keefer's study, the relationship between the seismic magnitude and the affected area can be expressed as following equation:

$$\log_{10}A = M - 3.46(\pm 0.47) \quad (2)$$

where A is the affected area in square kilometers, M is seismic magnitude for  $5.5 < M \leq 9.2$  (Keefer, 2002). Following this equation, the affected area during the Lushan earthquake is calculated to range in  $1175 \sim 10232 \text{ km}^2$ .

As to the Lushan earthquake, it is located in the southwestern China, where strong earthquakes triggered landslides were mainly located within the area with seismic intensity  $\geq \text{VII}$ . Also, in this region, the earthquakes with magnitude 7.0 can cause landslides distributed in an area ranging from 2,600 to 8,843  $\text{ km}^2$  (Chen et al., 2012). According to the Lushan earthquake seismic intensity map issued by the China Earthquake Administration, the area bounded by the seismic intensity line of VII is around  $5,655 \text{ km}^2$ .

In this study, landslide inventory obtained from interpretation of remote images indicates that the landslides are mainly distributed in the area with seismic intensity  $\geq \text{VII}$ . They are bounded by the semi-minor axis of intensity VII, but not extend to the south boundary end of the prolate axis (Fig. 9). The affected area is calculated to be  $2,200 \text{ km}^2$ .

Both the distance–magnitude (equation (1)) and magnitude–area (equation (2)) empirical relationships can be used to estimate how widely a given earthquake would influence. From this study, it seems that distance–magnitude relation is a good method to estimate the comparatively concentrated landslides affected area.

## 4.2 Criteria of the landslides size

As mentioned above, both the 2008 Ms8.0 Wenchuan earthquake and the 2013 Ms 7.0 Lushan earthquake occurred in the Longmen Shan fault zone in succession (Fig. 1, Fig. 12). The Wenchuan earthquake occurred at the north side of the Lushan earthquake, and the distance between these two epicenters is around 90 km. Unlike the Wenchuan earthquake, which generated a 240 km and a 90 km long ground surface ruptures (Xu et al., 2008; Yu et al., 2010), the Lushan earthquake has no obvious ground surface rupture.

Landslides spatial distribution during these two earthquakes both show the NE-SW extending direction the same as the LSFZ striking, this indicates the influence of causative faults. Although there may be many differences in the landslides triggered by the Lushan earthquake and the Wenchuan earthquake, the most distinct ones, which can be found from the landslide inventory map, should be the affected area and the amount of the landslides (Fig. 12).

As an essential part of seismic landslides hazard analysis, both the landslides affected area and landslides quantity are the criteria used to evaluate landslide hazard severity. Due to the lacking of the comparative strict definitions on the landslides, the quantity of landslides from different researchers usually shows enormous difference. Although some researches show that the landslide size has little influence on the distribution characteristics (Qi et al, 2012), sometimes landslide inventory can seriously influence statistics results especially when calculating LPD value. For example, on account of the researcher's subjective opinion about the definition of landslides or the remote images resolution, there exist obvious discrepancies in the quantity of landslides

triggered by the Wenchuan earthquake (Yin et al., 2009; Huang et al., 2009; Qi et al., 2010; Dai et al., 2011). The latest study shows that the number of the landslides triggered by the Wenchuan earthquake is up to 197,481 and they distributed in an area of about 110,000 km<sup>2</sup> (Xu et al., 2013a). It is obvious that using of the smallest amount of 15,000 individual landslides (Yin et al., 2009) and the biggest 197,481 will produce different results. Therefore, it becomes necessary and urgent to propose the interpretation standards for delimitating landslides.

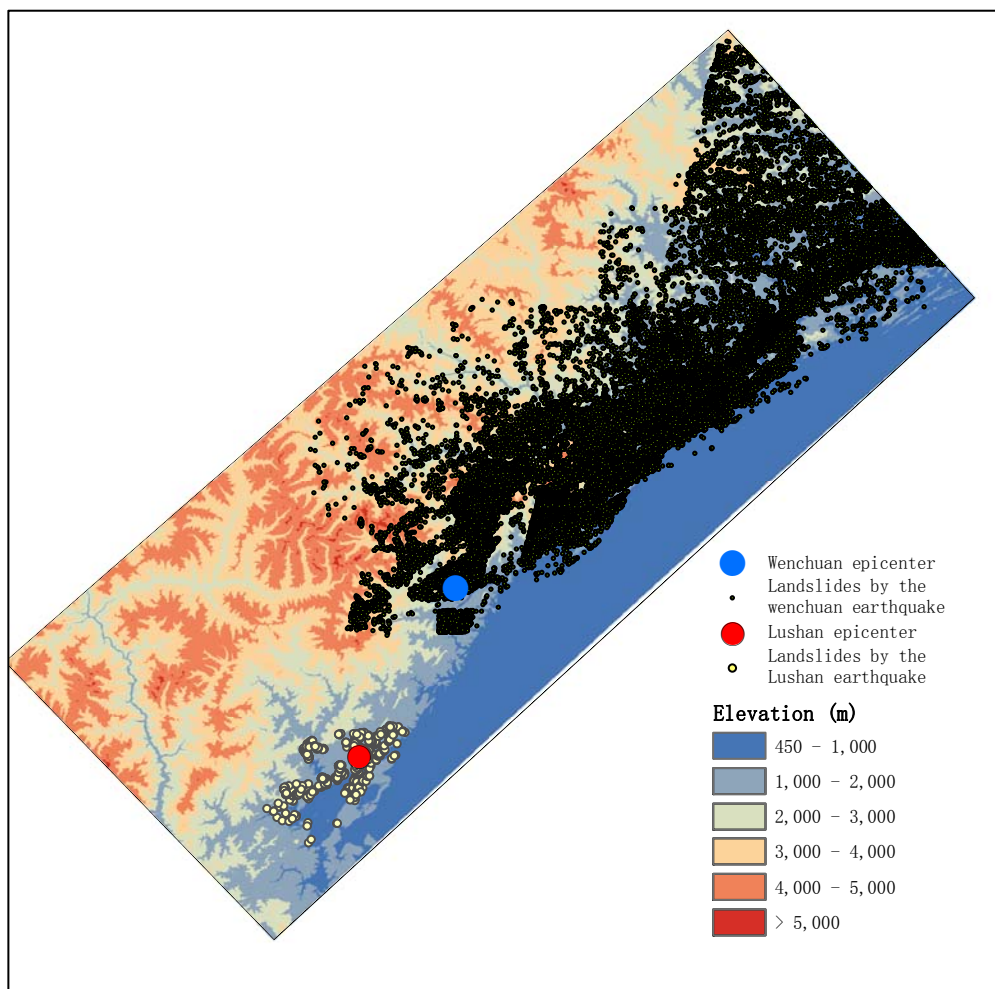


Fig. 12. Landslides distribution during the Wenchuan earthquake (Dai et al., 2011 ) and the Lushan earthquake

## 5. Conclusions

The Ms7.0 Lushan earthquake triggered more than 1,000 individual landslides in an area of 2,200 km<sup>2</sup>. Although landslide damages from the Lushan earthquake were not as serious as the Wenchuan earthquake, the landslides really blocked many roads and exacerbated the overall transportation problems in the mountainous region.

There is no ground surface rupture generated during the Lushan earthquake, nevertheless, the landslides spatial distribution still shows the domination from the causative faults. The landslides

are mainly concentrated around the epicenter and in scale with the seismic intensity. LPD decreases with the increasing distance from the epicenter, and more than 90 % of the landslides are located within 30 km from the epicenter.

Landslide distribution has a positive correlation with slope gradient. Higher LPD occur in the young strata systems composed of soft rocks like mudstone and sandstone. Plenty of landslides develop along the roads in the mountainous area and river banks. The man-made roads in the mountainous area become important factors which are needed to be taken account of when doing earthquake-triggered landslides assessments.

Also, it is concluded with a discussion that the distance-magnitude relation shows more precise in the estimation of landslides affected boundary during the Lushan earthquake, and standards for delimitating landslides when doing remote image interpretation are expected.

*Acknowledgements.* The authors are grateful the supports from National Key Technology R & D Program (Grant No. 2012BAK15B0103) and National Key Basic Research Program of China (Grant No.2013CB733205). Thanks the Institute of Remote Sensing and Digital Earth, China Academic Science for providing the remote images. The authors would like to give great thanks to the reviewers for their constructive and pertinent comments that greatly improved the quality of the manuscript.

## Reference

- Bommer, J. J., Carlos, E., and Rodríguez, C. R.: Earthquake-induced landslides in Central America, *Eng. Geol.*, 63, 189–220, 2002.
- Chen, X. L., Zhou Q., Ran H. L. and Dong R. S.: Earthquake-triggered landslides in southwest China, *Nat. Hazards Earth Syst. Sci.*, 12, 351–363, 2012.
- Chen X. L., Ran H. L. and Yang W. T.: Evaluation of factors controlling large earthquake-induced landslides by the Wenchuan earthquake. *Nat. Hazards Earth Syst. Sci.*, 12, 3645–3657, 2012
- China Geological Survey, CGS.: Regional geological map of Sichuan Province (1:200, 000), Geological Press, 2001.
- Dai F.C., Xu C., Yao X., Xu L., Tu X.B., and Gong Q.M.: Spatial distribution of landslides triggered by the 2008 Ms 8.0 Wenchuan earthquake, China, *Journal of Asian Earth Sciences*, 40, 883 – 895, 2011.
- Densmore, A., Ellis, A., Li, Y., Zhou R.J., Hancock G.S., and Richardson N.: Active tectonics of the Beichuan and Pengguan faults at the eastern margin of the Tibetan Plateau, *Tectonics*, 26, 1 – 17, 2007.
- Devkota, K. C., Regmi, A. D., Pourghasemi, H. R., Yoshida, K., Pradhan, B., Ryu, I., Dhital, M. R., and Althuwaynee, O.: Landslide susceptibility mapping using certainty factor, index of entropy and logistic regression models in GIS and their comparison at Mugling-Narayanghat road section in Nepal Himalaya, *Nat. Hazards*, 65, 135–165, 2013.
- Guzzetti, F., Mondini, A.C., Cardinali, M., Fiorucci, F., Santangelo, M., and Chang, .KT. : Landslide inventory maps: new tools for an old problem. *Earth Sci Rev.*, 112(1–2), 42–66, 2012
- Haeussler, P.J., Schwartz, D.P., Dawson, T.E., Stenner, H.D., Lienkaemper, J.J., Sherrod, B., Cinti, F.R., Montone, P., Craw, P.A., Crone, A.J., and Personius, S.F.: Surface Rupture and Slip Distribution of the Denali and Totschunda Faults in the 3 November 2002 M 7.9 Earthquake, *Bulletin of the Seismological Society of America*, 94, 23-52, 2004.
- Han, Z.J., Ren, Z.K., Wang, H. and Wang, M.M.: The surface rupture signs of the Lushan “4.20” Ms 7.0 earthquake at Longmen township, Lushan county and its discussion. *Seismology and geology*, 35(2), 388-397. 2013.
- Harp, E.L., Keefer, D.K., Sato, H.P., and Yagi, H.: Landslide inventories: the essential part of seismic landslide hazard analyses. *Engineering Geology*, 122 (1–2), 9–21, 2011.

- Highland, L.M., and Bobrowsky, Peter, 2008: The landslide handbook—A guide to understanding landslides: Reston, Virginia, U.S. Geological Survey Circular 1325, 129 p.
- Huang, R.Q. and Li, W. L.: A study on the development and distribution rules of geohazards triggered by “5.12” Wenchuan Earthquake, *Chinese Journal of rock mechanics and engineering*, 27 (12), 2585-2592, 2008 (in Chinese).
- Huang, R. Q., Pei, X. J., Zhang, W. F., Li, S. G. and Li, B. L.: Further examination on characteristics and formation mechanism of Daguangbao landslide, *Journal of Engineering Geology*, 17(6), 725-736, 2010 (in Chinese).
- Jibson, R.W., Harp, E.L., Schulz, W. and Keefer, D.K.: Landslides triggered by the 2002 M-7.9 Denali Fault, Alaska, earthquake and the inferred nature of the strong shaking, *Earthquake Spectra*, 20, 669-691, 2004.
- Kawabe, H. Earthquake and earthquake motion. In: Nakamura H., Tsuchiya S., Inoue K. & Ishikawa Y. eds. *Earthquake Sabo* (in Japanese). Kokon Shoin, Tokyo, 2000. 1~13.
- Keefer, D. K.: Landslides caused by earthquakes, *Geological Society of America Bulletin*, 95,406-421, 1984.
- Keefer, D.K.: Investigating landslides caused by earthquakes—a historical review, *Surveys in Geophysics*, 23, 473-510, 2002.
- Khazai, B. and Sitar, N.: Evaluation of factors controlling earthquake-induced landslides caused by Chi-Chi earthquake and comparison with the Northridge and Loma Prieta events, *Engineering Geology*, 71, 79–95, 2003.
- Meunier, P., Hovius, N. and Haines, J.A.: Regional patterns of earthquake-triggered landslides and their relation to ground motion, *Geophys. Res. Lett.*, 34, L20408, doi:10.1029/2007GL031337, 2007.
- Qi, S. W., Xu Q., Lan H. X., Zhang B. and Liu J.Y.: Spatial distribution analysis of landslides triggered by 2008.5.12 Wenchuan Earthquake, China, *Engineering Geology*, 116, 95-108, 2010.
- Qi, S. W., Xu, Q., Lan, H. X., Zhang, B., Liu, J. Y. 2012. Resonance effect existence or not for landslides triggered by 2008 Wenchuan, *Engineering Geology*, 151: 128-130.
- Ramakrishnan, D., Singh, T. N., Verma, A. K., Gulati, A., and Tiwari, K. C.: Soft computing and GIS for landslide susceptibility assessment in Tawaghat area, Kumaon Himalaya, India, *Nat.Hazards*, 65, 315–330, 2013.
- Rodríguez C.E., Bommerb J.J. and Chandlerb R.J.: Earthquake-induced landslides: 1980–1997, *Soil Dynamics and Earthquake Engineering*, 18, 325–346, 1999.
- Simonett, D.S.: Landslide distribution and earthquakes in the Bewani and Torricelli Mountains, New Guinea, statistical analysis. In Jennings, J.N. and Mabbutt, J.A., eds., *Landform Studies from Australia and New Guinea*, Cambridge, Cambridge University Press, 64-84, 1967.
- Wang H. B., Sassa K. and Xu W. Y.: Analysis of a spatial distribution of landslides triggered by the 2004 Chuetsu earthquakes of Niigata Prefecture, Japan, *Nat Hazards*, 41, 43-60, 2007.
- Wang W. N., Wu H. L., Nakamura H., Wu S. C., Ouyang S. and Yu M. F.: Mass movements caused by recent tectonic activity: The 1999 Chi-chi earthquake in central Taiwan, *The Island Arc*, 12,325–334, 2003.
- Wen, B. P., Wang, S. J., Wang, E. Z., Zhang, J. M.: Characteristics of rapid giant landslides in China, *Landslides*. 4(3), 247–261, 2004.
- Xu, C., Xu, X.W., Yao, Q. and Wang, Y.Y.: GIS-based bivariate statistical modeling for earthquake-triggered landslides susceptibility mapping related to the 2008 Wenchuan earthquake, China. *Quarterly Journal of Engineering Geology and Hydrogeology*, doi:10.1144/qjegh2012-006, 2013.
- Xu, Q. and Li, W. L.: Distribution of large scale landslides induced by the Wenchuan earthquake, *Journal of Engineering Geology*, 18(6), 818-826, 2010 (in Chinese).
- Xu, X.W., Wen, X.Z., Ye, J.Q., Ma, B.Q., Chen, J., Zhou, R.J., He, H.L., Tian, Q.J., He, Y.L., Wang, Z.C., Sun, Z.M., Feng, X.J., Yu, G.H., Chen, L.C., Chen, G.H., Yu, S.E., Ran, Y.K., Li, X.G., Li, C.X., An, Y.F.: The Ms 8.0 Wenchuan earthquake surface ruptures and its seismogenic structure. *Seismology and Geology* 30 (3), 597 – 629, 2008.

- Xu X. W., Wen X. Z., Han Z. J., Chen G. H., Li C. Y., Zheng W. J., Zhang S.M., Ren Z.K., Xu C., Tan X.Y., Wang M.M., Ren J.J., He Z. and Liang M.J. Lushan Ms7.0 earthquake: A blind reverse-fault event. *Chin. Sci. Bull.* 58. 2013. doi: 10.1007/s11434-013-5999-4.
- Yin, Y. P., Wang, F. W. and Sun, P.: Landslide hazards triggered by the 2008 Wenchuan earthquake, Sichuan, China, *Landslides*, 6(2), 139–152, 2009.
- Yu, G. H., Xu X. W., Klinger Y., Diao G. L., Chen G. H., Feng X. D., Li C. X., Zhu A. L., Yuan R. M., Guo T. T., Sun X. Z., Tan X. B. and An Y. F.: 2010. Fault-Scarp Features and Cascading-Rupture Model for the Mw 7.9 Wenchuan Earthquake, Eastern Tibetan Plateau, China, *Bulletin of the Seismological Society of America*, 100, 2590-2614, doi:10.1785/0120090255, 2010.
- Zhang, P.Z., Wen, X.Z., Shen, Z.K. and Chen, J.H.: Oblique, High-Angle, Listric-Reverse Faulting and Associated Development of Strain: The Wenchuan Earthquake of May 12, 2008, Sichuan, China. *Annu. Rev. Earth Planet. Sci.* 38, 353-382, 2010.